INTERNATIONAL JOURNAL OF HYDROGEN ENERGY XXX (2016) 1–8

Available online at www.sciencedirect.com

ScienceDirect

journal homepage: www.elsevier.com/locate/he

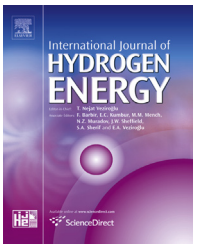

Numerical analysis of microwave assisted thermocatalytic decomposition of methane

Siddharth Gadkari [a], *Beatriz Fidalgo* [b,**], *Sai Gu* [a,*]

[a] *Department of Chemical and Process Engineering, University of Surrey, Guildford GU2 7XH, United Kingdom*
[b] *School of Energy, Environmental Technology and Agrifood, Cranfield University, Bedfordshire MK43 0AL, United Kingdom*

ARTICLE INFO

Article history:
Received 16 August 2016
Received in revised form
7 September 2016
Accepted 17 September 2016
Available online xxx

Keywords:
Thermocatalytic decomposition of methane
Microwave heating
Activated carbon
Coupled numerical model
Hydrogen

ABSTRACT

A comprehensive 3D coupled mathematical model is developed to study the microwave assisted thermocatalytic decomposition of methane with activated carbon as the catalyst. A simple reaction kinetic model for methane conversion (accounting for catalyst deactivation) is developed from previously published experimental data and coupled with the governing equations for the microwaves, heat transfer, mass transfer and fluid flow physics. Temperature distribution and concentration profiles of CH_4 & H_2 in the catalyst bed are presented. The temperature profiles at different input power values predict a non-uniform temperature distribution with hot-spots near the top and bottom of the catalyst. The concentration profiles predict a linear variation of CH_4 and H_2 concentration along the length of the reactor and show a good agreement with experimental conversion values. The influence of volumetric hourly space velocity on methane conversion is also investigated.

Introduction

Global concern over the increasing level of greenhouse gas emissions and the associated climate change has driven the search for renewable and more environment friendly sources of fuels [1]. Hydrogen, which has a high heating value and water as its only combustion product, is being considered as an ideal alternative to the traditional fossil fuels [2]. However, as there are no natural sources of hydrogen in elemental form, different methods are employed to extract H_2 from various compounds. Almost 50% of the commercial hydrogen is being produced from natural gas (whose main component is methane) using the steam methane reforming (SMR) process [3]. Compared to other processes, such as partial oxidation and coal gasification, SMR is more efficient (50%), however it generates large quantities of COx emissions and additional separation steps are required to obtain pure H_2 before it can be used in fuel cells [4]. Thermocatalytic decomposition (TCD) of methane as described in Eq. (1), is a promising alternative to SMR as it can produce hydrogen without any direct COx emissions [4].

$$CH_4 \rightarrow C + 2H_2 \quad \Delta H_o = +75 kJ/mole \tag{1}$$

As TCD of methane is an endothermic process, catalysts are typically used to expedite the kinetics and reduce the required temperature. A wide range of metal catalysts (Ni, Co, Fe and their alloys) have been used for methane TCD and have shown high activity, however catalyst deactivation by carbon deposition on

* *Corresponding author.*
** *Corresponding author.*
E-mail address: sai.gu@surrey.ac.uk (S. Gu).

http://dx.doi.org/10.1016/j.ijhydene.2016.09.126

Nomenclature

k_{d_0}	Pre-exponential factor, $[mol/m^3]^m\ s^{m-1}$
E_d	Activation Energy, J/mol
c_p	Specific Heat Capacity, J/kg K
E	Electric Field, V/m
H	Magnetic Field, A/m
T	Temperature, K
Q	Heat Source, W/m^3
Q_f	Flow rate, m^3/s
c_i	Concentration of Species, mol/m^3
N_i	Mass Flux of Species, kg/m^2 s
u	Velocity, m/s
p_i	Pressure of Species, Pa
f	frequency, 1/s
a	Activity, dimensionless
d	Activity exponent, dimensionless
m	VHSV exponent, dimensionless
k	Thermal Conductivity, W/m K
h	Heat transfer coefficient, $W/(m^2\ K)$
D_i	Diffusion Coefficient of Species, m^2/s
D_e	Effective Diffusion Coefficient, m^2/s
R	Universal Gas Constant
ρ	Density, kg/m^3
ε_p	Porosity, dimensionless
σ	Electrical Conductivity, S/m
μ	Dynamic Viscosity, Pa s
ε_r	Relative Permittivity, dimensionless
μ_r	Relative Permeability, dimensionless
k_0	Wave number of free space
ε_0	Permittivity of free space
κ	Permeability, m^2
ω	Angular Frequency, Hz
ε_e	emissivity, dimensionless

Subscript

in	inlet
p	porous catalyst
i	chemical species, CH_4, H_2 or C
0	initial
eff	effective value

the surface is still a major concern [5]. In the last decade several researchers evaluated carbonaceous catalysts such as activated carbon and carbon black for TCD [6–14]. With numerous advantages such as, low cost, resistance to high temperature, easy availability, resistance to poisoning by sulfur and other harmful impurities in the feedstock, etc., the carbonaceous catalysts have spurred several investigations to thoroughly understand the catalytic reaction mechanism [6–14]. In addition, unconventional heating methods such as heating via microwave irradiation are also being evaluated for process intensification in heterogeneous catalytic reactions [15–20]. Contrary to conventional heat sources, microwave heating provides several advantages including 1) uniform volumetric heating, 2) comparatively high heating rate, 3) better selectivity, 4) heating without contact, and 5) short start-up or stopping time [16,17]. Thus microwave heating is not only being studied for decomposition of methane but also for many other heterogeneous chemical reactions such as dry and steam reforming of methane, coal and biomass pyrolysis, methanol steam reforming, methanol oxidation, hydrogen evolution from organic hydrides, water gas shift reaction, etc [17–28]. Dominguez et al. [21], combined microwave heating as a heat source and activated carbon as the catalyst for the thermocatalytic decomposition of methane in a fixed bed quartz-tube flow reactor. Their results showed higher conversions of methane for microwave heating compared to conventional electric heating. These differences in conversion have been attributed to the formation of hot spots and synergetic effects due to microwave irradiation [21]. However the exact mechanisms are still unclear. Extensive research needs to be carried out to thoroughly understand the microwave assisted biochemical conversion processes. While there have been several experimental studies, the number of numerical studies is comparatively far less [29]. Chen et al. [29] investigated the influences of microwave power, volumetric hourly space velocity (VHSV), and catalyst bed geometry on the performance of microwave assisted TCD using a 2D mathematical model. However they have used the reaction kinetic mechanism derived for TCD of methane using conventional heating sources. The experimental comparison shown in their paper is thus non-conclusive. Additionally the 2D model used by Chen et al. [29] does not provide information on the temperature and concentration profiles in the central volume of the reactor and also fails to describe the influence of hot spots. The goal of the current study is to develop a comprehensive 3D model for the microwave-assisted decomposition of methane and provide a better understanding of the interactions between the chemical and physical mechanisms governing this process. A simple kinetic mechanism for the decomposition of methane and catalyst deactivation has also been developed using the experimental data of Dominguez et al. [21], and has been used to predict the concentration distributions in the reactor. In addition the effect of VHSV on the methane TCD process is also investigated.

Model formulation

Geometry

A multimode microwave oven operating at a frequency of 2.45 GHz was considered for this model. Microwave radiation is directed from the magnetron to the cavity through a rectangular waveguide operating in the TE_{10} mode. The walls of the oven and the waveguide are assumed to be made of copper. The reactor tube is made of quartz and placed at the center of the microwave cavity. Only the section of the reactor tube filled with the activated carbon catalyst is considered in the model, as it is assumed that the reaction only occurs in the presence of catalyst.

In order to reduce the computational expense of the numerical analysis, a symmetry cut is applied vertically through the center of the oven, waveguide and the reactor tube. The schematic of the final reaction system used in the model is shown in Fig. 1, along with the dimensions for the microwave cavity and the waveguide. The dimensions of reactor tube are 2.1 cm diameter and 6 cm height.

To present a more general system, the dimensions of the microwave device used in this study are different from those of

Please cite this article in press as: Gadkari S, et al., Numerical analysis of microwave assisted thermocatalytic decomposition of methane, International Journal of Hydrogen Energy (2016), http://dx.doi.org/10.1016/j.ijhydene.2016.09.126

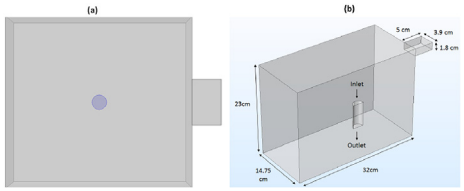

Fig. 1 – Schematic of the (a) top view of the full microwave cavity with the reactor tube at the center and (b) symmetrical geometry used in the model.

the microwave cavity used in Dominguez et al. [21]. However the section of the reactor tube represented here is equal to the volume of the catalyst considered by Dominguez et al. [21]. By maintaining the catalyst volume and the average temperature, it is assumed that the specific energy consumption of the catalytic bed would be similar and the overall decomposition performance over the catalyst would be the same regardless of the geometry of microwave device used [30].

Governing equations

Governing equations for the microwaves, heat transfer, species transport (mass transfer) and fluid flow through the porous catalyst are represented by Eqs. (2)–(6).

$$\nabla \times (\mu_r^{-1} \nabla \times E) - k_0^2 \left(\varepsilon_r - \frac{j\sigma}{\omega \varepsilon_0} \right) E = 0 \tag{2}$$

$$(\rho C_p)_{eff} \frac{\partial T}{\partial t} + \rho C_p u \cdot \nabla T = \nabla . (k_{eff} \nabla T) + Q \tag{3}$$

$$\varepsilon_p \frac{\partial c_i}{\partial t} + \nabla \cdot (-D_{e,i} \nabla c_i) + \nabla (u c_i) = R_i \tag{4}$$

$$\frac{\rho}{\varepsilon_p} \left(\frac{\partial u}{\partial t} + (u \cdot \nabla) \frac{u}{\varepsilon_p} \right) = -\nabla \cdot p +$$

$$\nabla \cdot \left[\frac{1}{\varepsilon_p} \left(\mu (\nabla u + \nabla u^T) - \frac{2}{3} \mu (\nabla \cdot u) I \right) \right] - (\kappa^{-1} \mu) u \tag{5}$$

$$\frac{\partial}{\partial t} (\varepsilon_p \rho) + \nabla \cdot (\rho u) = 0 \tag{6}$$

The wave number of free space, k_0 is defined as $k_0 = \omega / c_0$, where c_0 is the speed of light in vacuum.

The heat source term, Q in the energy balance equation is calculated from the volumetric power generated by dielectric heat dissipation in the biomass sample due to microwave exposure and is expressed as:

$$Q = 2\pi f \varepsilon_0 \varepsilon'' |E|^2 \tag{7}$$

Also the effective heat capacity and conductivity values are defined as

$$(\rho C_p)_{eff} = (1 - \varepsilon_p) \rho_p C_{p,p} + \varepsilon_p \rho C_p \tag{8}$$

$$k_{eff} = (1 - \varepsilon_p) k_p + \varepsilon_p k \tag{9}$$

The complex dielectric constant is defined as, $\varepsilon_r = \varepsilon' - i\varepsilon''$

where, ε' represents the dielectric constant, ε'' the dielectric loss factor, μ_r the relative permeability, E the electric field vector, j the imaginary unit, σ the conductivity, ω the angular frequency, ε_0 is permittivity of free space, f the frequency, ρ the density, C_p the heat capacity, T the temperature, u the velocity vector, k the conductivity, Q the heat source due to microwaves, ε_p the porosity, c_i the concentration of individual species, i represents either methane gas, hydrogen gas or carbon, D_e the diffusion coefficient, R_i the species' net reaction rate, p the pressure, μ the dynamic viscosity, I the identity matrix. Subscript p refers to the quantities of the porous catalyst.

Eq. (2) which calculates the electric field vector E is solved at a particular frequency of 2.45 GHz in the whole system which includes the microwave oven cavity, waveguide and the reactor tube. Eqs. (3)–(6) are solved in a transient study to obtain the temperature, velocity, pressure and species concentration profiles in the reactor tube.

The governing equations are coupled to each other through the variables. For example, the heat source term couples the energy balance and microwave equations. The temperature value obtained from the energy balance equation is coupled to the reaction kinetics. The species concentrations obtained from the kinetic model are coupled to the mass transfer equation. The velocity and pressure profiles obtained by solving the momentum transfer (5) and continuity (6) equations are coupled to the mass transfer and heat transfer physics.

Once the catalyst reaches the required temperature, pure methane gas (CH_4) enters into the reactor tube from the top and decomposes into carbon (C) and hydrogen (H_2) following the kinetics described in the next section. The solid carbon formed during the reaction is deposited on the catalyst. Thus the gas pressure in the reactor is expressed only as a function of methane and hydrogen, as per Eq. (10).

$$p = RT(c_{CH_4} + c_{H_2}) \tag{10}$$

All the input parameters that are used in the model are presented in Table 1.

The coupled governing equations were solved using Finite Element Method in COMSOL Multiphysics v 5.0. Eq. (2) was solved at a fixed frequency value of 2.45 GHz using the FGMRES Iterative Solver which uses the restarted flexible generalized minimum residual method. Eqs. (3)–(6) were solved in a transient study performed using the PARDISO solver with a nested dissection multithreaded pre-ordering algorithm.

Chemical reaction kinetics

Activity (a) of the catalyst is assumed to be decreasing linearly with time as the amount of carbon deposited grows, and is defined as [41]:

$$a = 1 - \frac{C(t)_{dep}}{C_{cm}} \tag{11}$$

where C_{dep} is the carbon deposited and C_{cm} is the maximum carbon deposited.

The catalyst activity is a direct function of operating conditions. Dominguez et al. [21] have studied the effect of

Please cite this article in press as: Gadkari S, et al., Numerical analysis of microwave assisted thermocatalytic decomposition of methane, International Journal of Hydrogen Energy (2016), http://dx.doi.org/10.1016/j.ijhydene.2016.09.126

Table 1 – Input parameters (material property values) used in the model.

c_{in}	41.6 mol/m^3	[21]
ρ	0.68 kg/m^3	[31]
c_p	815 J/kg K	[31]
k	0.02 W/(m °C)	[31]
c_{p_p}	800 J/kg K	[32]
ρ_p	490 kg/m^3	[33]
k_p	30 W/(m K)	[21]
ε_p	0.68	[33]
h	5 W/(m^2 K)	Estimated
ω_e	0.9 W/(m^2 K)	[34]
D_{CH_4}	1e-7 m^2/s	[35]
D_{H_2}	4e-7 m^2/s	[35]
ε_r (Catalyst, Microwave Cavity)	25-30i, 1	[35–38]
μ_r (Catalyst, Microwave Cavity)	0.91+ 0.08i, 1	[35,39]
σ (Catalyst, Microwave Cavity)	45, 0 S/m	[35,40]

temperature and volumetric hourly space velocity (VHSV) on methane conversion, while keeping the inlet CH_4 concentration constant.

The deactivation rate of the catalyst, in terms of Arrhenius temperature and VHSV dependency can thus be described as:

$$-\frac{da}{dt} = k_d \mathrm{VHSV}^m a^d = k_{d_0} e^{-E_d/RT} \mathrm{VHSV}^m a^d \tag{12}$$

where k_{d_0} and E_d are the pre-exponential factor and activation energy for the deactivation reaction rate and m & d are exponents for the VHSV and activity respectively.

Different values of d (0, 0.5, 1 & 2) were considered and the corresponding values of k_{d_0}, E_d and m were calculated. These values were then substituted in Eq. (12) to predict the activity values as a function of time. These predicted values were compared with experimental values determined from Eq. (11) using the data of Dominguez et al. [21].

d = 0.5 was found to produce the best agreement between predicted and experimental values of activity.

In the case of d = 0.5, activity can be expressed as,

$$a^{0.5} = 1 - 0.5 k_d \mathrm{VHSV}^m t = 1 - 0.5 k_{d_0} e^{-E_d/RT} \mathrm{VHSV}^m t \tag{13}$$

Here VHSV is given in m^3/(mol s), E_d is given in J/mol, T is in K and k_{d_0} in [mol/m^3]^m s^{m-1}.

The values of k_{d_0}, E_d and m for d = 0.5, were derived as: $m = 0.14$, $k_{d_0} = 9.82 \times 10^{-4}$ and $E_d = 2844$.

Following Abbas and Daud [41] activity can also be defined as:

$$a = \frac{r_c}{r_0} \tag{14}$$

$$r_c = \frac{dC}{dt} \tag{15}$$

where r_c is the rate of carbon formation (given as mol/m^3 s), r_0 is the initial rate of carbon formation (given as mol/m^3 s) and C is the carbon deposited in mol/m^3.

Based on the experimental data of Dominguez et al. [21], r_0 is derived as a function of T and VHSV as,

$$r_0 = 7e^{-4} \cdot T + 970937 \cdot \mathrm{VHSV} - 0.1053 \tag{16}$$

where r_0 is given in mol/m^3 s, T in K and VHSV in m^3/mol s.

Kinetics is implemented into the model in terms of rate of change of different species concentrations as:

$$r_c = r_0 \cdot a = \frac{dC}{dt} = \frac{1}{2}\frac{dH_2}{dt} = -\frac{dCH_4}{dt} \tag{17}$$

with a being calculated by solving Eq. (12) for d = 0.5.

It should be noted that the kinetic model developed here is based on limited data set and thus is only applicable for the set of conditions used by Dominguez et al. [21]. The aim of the current work is to demonstrate the applicability of 3D coupled models for studying microwave assisted TCD of methane. Thus the necessity of using the above kinetic model, even with its limited applicability, is reasonable.

Boundary conditions

Walls of the microwave cavity and the waveguide are considered to be made of copper in this model and thus the electric field will only penetrate short distance outside the boundary. This penetration is accounted using a useful approximation known as the impedance boundary condition (IBD), which avoids the need to include another domain in the model while ensuring even the small losses are accounted [35]. IBD is expressed as,

$$\sqrt{\frac{\mu_0 \mu_r}{\varepsilon_0 \varepsilon_r - j\sigma/\omega}}\, n \times H + E - (n \cdot E) n = 0 \tag{18}$$

where n is the unit normal, H is the magnetic field.

At the symmetrical boundary, electric current cannot flow and the tangential magnetic field vanishes, this is represented as following,

$$n \times H = 0 \tag{19}$$

At the entrance of the rectangular waveguide, the applied input power value is specified,

$$P = P_0 \tag{20}$$

The temperature gradient across the symmetrical boundary is zero, which is implemented by the following boundary condition

$$n \cdot (k \nabla \mathrm{T}) = 0 \tag{21}$$

The outer surface of the reactor tube loses heat due to convection and radiation. These losses are represented as,

$$n \cdot (k \nabla \mathrm{T}) = h(\mathrm{T}_0 - \mathrm{T}) + \varepsilon_e \sigma_{sb} (\mathrm{T}_0^4 - \mathrm{T}^4) \tag{22}$$

where, h is the heat transfer coefficient and ε_e is the emissivity of the reactor tube.

At the inlet of the reactor tube, the flow rate is specified as,

$$Q_f = Q_{f_{in}} \tag{23}$$

At the outlet of the reactor tube the pressure condition is applied as,

$$p = 0 \tag{24}$$

At the symmetrical boundary, vanishing shear stresses and no penetration condition is implemented as following

$$u \cdot n = 0 \quad \text{and} \quad K - (K \cdot n) n = 0 \tag{25}$$

where $K = \mu(\nabla \mathrm{u} + \nabla \mathrm{u}^{\mathrm{T}}) n$

Please cite this article in press as: Gadkari S, et al., Numerical analysis of microwave assisted thermocatalytic decomposition of methane, International Journal of Hydrogen Energy (2016), http://dx.doi.org/10.1016/j.ijhydene.2016.09.126

At the top boundary or inlet of the reactor tube, the inlet concentration of CH_4 is specified as,

$$c_{CH_4} = c_{in} \tag{26}$$

At the outlet of the reactor tube, the diffusive transport can be ignored as convection is the dominant mode of transport mechanism and this is implemented as following

$$n\cdot(-D_i\nabla c_i) = 0 \tag{27}$$

At the symmetrical boundary, there is no mass flux in the normal direction across the boundary, implemented as follows,

$$-n\cdot N_i = 0 \tag{28}$$

Results and discussion

Electric field and temperature profiles

Fig. 2 shows the normal electric field distribution in the microwave cavity, with and without the reactor tube (with the activated carbon catalyst), for applied input power of $P_0 = 1400$ W. The electric field distribution depends on the geometry of the cavity and the waveguide, as well as on the position of the waveguide. As can be seen from Fig. 2 the electric field within this multimode microwave cavity is a complex standing wave with several modes resulting in a non-uniform field distribution with areas of low and high microwave energy. Introduction of the reactor tube (catalyst) alters the electric field distribution inside the cavity as can be clearly seen by comparing plots A and B from Fig. 2. Absorption of microwave energy by the catalyst and the reflections from the walls of the microwave cavity redistribute the electromagnetic field. This also explains the importance of the position of any sample inside the cavity, as not all regions are exposed to equal field intensity.

Once the sample is exposed to the electromagnetic waves, it gets heated up due to the continuous re-alignment of molecular dipoles which is restrained by the inter-molecular bonds and leads to molecular friction. Geometry of the microwave cavity, position and geometry of the catalyst and its dielectric and thermal properties determine how the sample gets heated on exposure to microwave radiation. The rate and intensity of the microwave heating are dependent on the complex relative permittivity, the dielectric loss tangent of the catalyst and the applied input power.

For a fixed position of the catalyst inside the microwave cavity, the average temperature of the catalyst can be changed by changing the input power. Once the power is switched on, the temperature in the catalyst increases and reaches a steady state in about 60 s in our simulations. Fig. 3 shows the steady state temperature distributions in the catalyst for three different applied input power values, $P_0 = 800$ W, $P_0 = 1000$ W and $P_0 = 1200$ W.

The average temperature of the catalyst increases with increase in input power as can be seen by comparing profiles A, B & C in Fig. 3. The temperature distribution is non-uniform over the catalyst, however the heating pattern appears to be similar for all input powers, with two hot spots being formed in the volume of the catalyst, one in the upper half closer to the top and the other in the lower half near the bottom. The center of the catalyst remains at a slightly lower temperature for all the three cases. The overall temperature difference in the catalyst for any value of input power is not more than 200 °C. The formation of hot spots depends on a number of factors including, the electromagnetic field in the microwave cavity, shape of the sample, the position of the sample in the microwave cavity, microscopic details of the porous structure and the dielectric properties of the catalyst. The properties of the activated carbon catalyst (which are also a function of temperature) change as the byproduct carbon from the reaction gets deposited on its surface over time. However these variations in the properties have not been included in the current model for simplification and due to lack of the availability of accurate temperature functions.

Comparison with experimental results

Once the catalyst reaches the required average temperature, pure methane gas enters the reactor tube from the top and decomposes into solid carbon and hydrogen gas. In the current study, the reaction rate and catalyst deactivation parameters have been derived from the experimental data from Dominguez et al. [21]. Fig. 4 shows the comparison between CH_4 conversion profiles as predicted from the simulation results at 800 °C and 900 °C and experimental results published in Dominguez et al. [21]. The conversion of CH_4 was calculated employing the concentrations of hydrogen and methane at the outlet of the catalytic bed similar to the procedure followed by Dominguez et al. [21]. The expression used for calculation of CH_4 conversion (%) is given by Eq. (29).

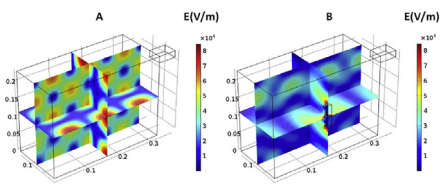

Fig. 2 – Normal electric field distribution in the microwave oven cavity (A) without the reactor tube (B) with the reactor tube.

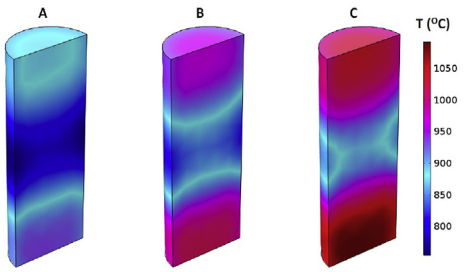

Fig. 3 – Temperature profile in the catalyst at applied power, (a) 800 W, (b) 1000 W and (c) 1200 W.

Please cite this article in press as: Gadkari S, et al., Numerical analysis of microwave assisted thermocatalytic decomposition of methane, International Journal of Hydrogen Energy (2016), http://dx.doi.org/10.1016/j.ijhydene.2016.09.126

$$CH_4\% = \frac{100 \times [\text{average}(H_2)_{out}/2]}{[\text{average}(CH_4)_{out} + \text{average}(H_2)_{out}/2]} \quad (29)$$

The simulation profiles at 800 °C and 900 °C, as can be seen in Fig. 4, do not completely overlap the experimental data, however there is still a fair agreement between the two. The predicted profiles show much better agreement at the higher temperature, 900 °C, while over-predict the CH_4 conversion (or under-predict the deactivation) at 800 °C.

Accounting for the fact that very limited experimental data was available for deriving the kinetic parameters, the agreement between simulation predictions and the experimental data can be considered good. This also suggests that the coupled CFD model can be reliably used for studying the microwave-assisted thermocatalytic decomposition of methane.

CH_4 and H_2 concentration profiles

Fig. 5 shows 3D volume and slice plots of the percentage concentration profiles of CH_4 and H_2 in the reactor tube after 1 min, 15 min and 30 min, at average catalyst temperature of 800 °C. As can be seen from Fig. 5 (a), the CH_4 decomposition starts immediately as it comes in contact with the catalyst at 800 °C. As the plots show, after 1 min, the concentration of CH_4 at the outlet falls to about 0–10 % and at the same time, the concentration of H_2 is between 90 and 100% at the outlet (Fig. 5 (b)). This is consistent with the experimental results which show a near 100% conversion of CH_4 as the input gas enters the reactor tube [21]. As the reaction proceeds further, the solid carbon which is being formed as a by-product of the reaction, gets deposited on the catalyst surface and blocks the active sites, which leads to decrease in the activity of the catalyst. This deactivation effect has been included in the kinetic model and accordingly the simulation results predict a decrease in CH_4 conversion overtime. This can be seen in terms of increase in CH_4 percentage and decrease in H_2 percentage at the outlet, as observed in the plots for 15 min and 30 min in Fig. 5. After 15 min the concentration of CH_4 at the outlet is about 20% and after 30 min it rises to about 35%. Corresponding H_2 concentration values at the outlet, as described in Fig. 5 (b), also accurately reflect the falling CH_4 conversion, which is consistent with the conversion profile at 800 °C as shown in Fig. 4 (a).

It should be noted that, though the temperature distribution in the catalyst volume is non-uniform, there is no sudden spike change in concentration value of either CH_4 and H_2 and the concentrations are varying linearly across the length of the reactor tube (the slice plots are shown for better visibility along the length of the catalyst). This suggests that the effect of temperature hot spots observed in Fig. 3 is quite local and the catalyst is heated volumetrically throughout the catalyst.

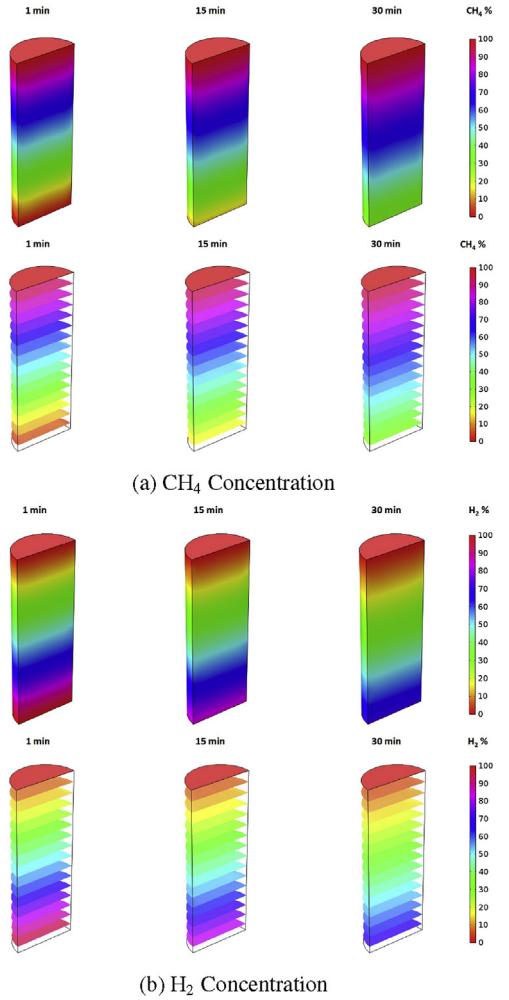

Fig. 5 – (a) CH_4 and (b) H_2 concentration distribution in terms of volume and slice plots in the reactor tube for average temperature of 800 °C at different times, t = 1 min, t = 15 min and t = 30 min.

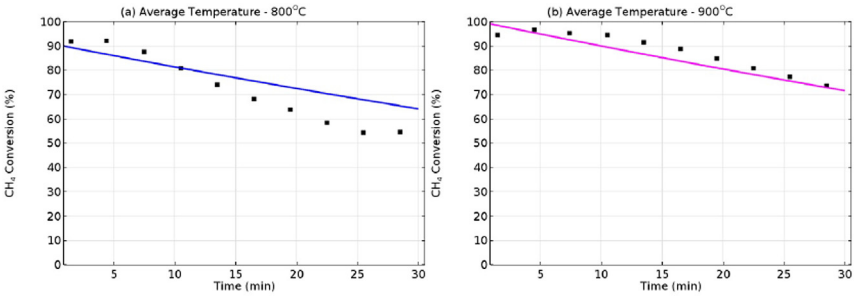

Fig. 4 – Comparison of experimental data (square markers) and simulation predictions (continuous lines) for CH_4 conversion as a function of time.

Please cite this article in press as: Gadkari S, et al., Numerical analysis of microwave assisted thermocatalytic decomposition of methane, International Journal of Hydrogen Energy (2016), http://dx.doi.org/10.1016/j.ijhydene.2016.09.126

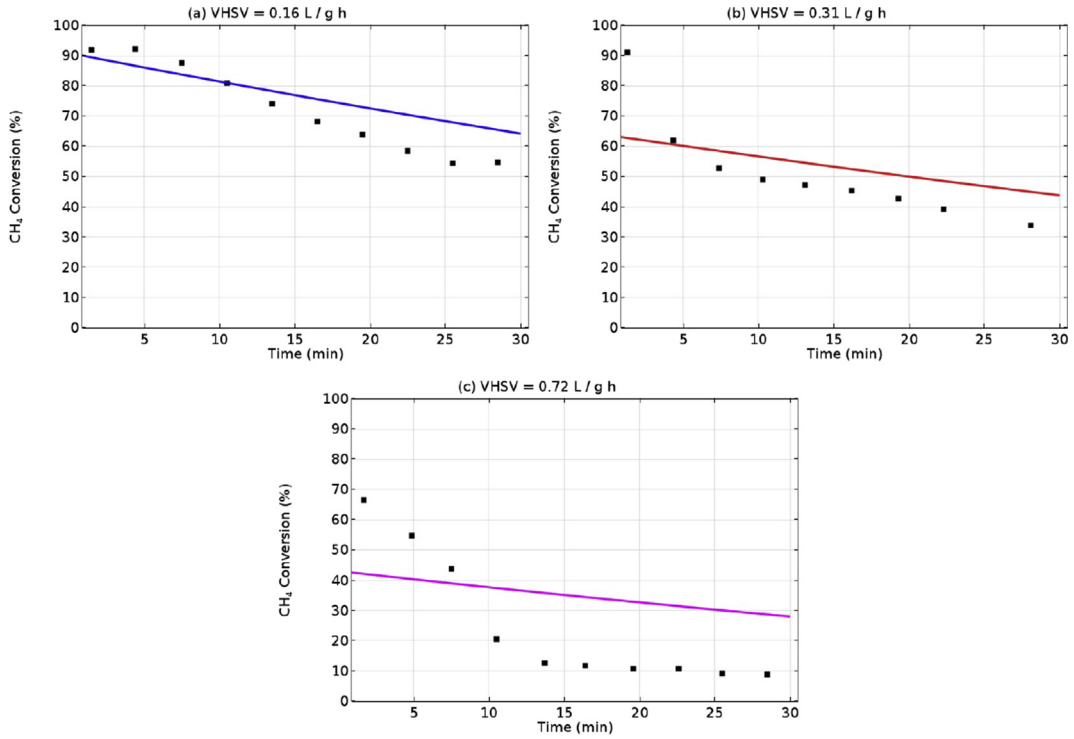

Fig. 6 – CH_4 conversion as a function of time for three different VHSV values, (A) 0.16 L/(g h), (B) 0.31 L/(g h) and (C) 0.72 L/(g h). Square markers represent the experimental data and continuous lines represent the simulation predictions.

Effect of volumetric hourly space velocity (VHSV) on conversion

Volumetric hourly space velocity or VHSV is defined as the ratio of the total volumetric flow rate at the inlet of the reactor to the mass of catalyst and it has been shown to influence the methane conversion [21]. The influence of VHSV was studied using the current model under the same conditions as used by Dominguez et al. [21], which essentially includes varying the VHSV by changing the flow rate of CH_4 and mass of catalyst at an average temperature of 800 °C. Fig. 6 shows the CH_4 conversion rates for the three different VHSV values, (a) 0.16 L/g h, (b) 0.31 L/g h and (c) 0.72 L/g h. Also included in the figures are the corresponding experimental values obtained by Dominguez et al. [21].

As can be seen in Fig. 6, the agreement between predicted and experimental CH_4 conversion values is good at lower VHSV values. However the agreement impairs as the VHSV value increases. At the highest VHSV value, 0.72 L/g h, simulation results under-predict the CH_4 conversion for the initial 10 min. Further down, the predicted values fail to predict the sudden drop in conversion as observed in experiments. The main reason for this disagreement is the lack of adequate experimental data to derive the correct correlation coefficient between the rate of reaction and VHSV. Nevertheless, the model does manage to capture the general trend and in accordance with previous findings by Dominguez et al. [21] and Chen et al. [29], the overall CH_4 conversion decreases with increase in VHSV. As the residence time of methane over the catalyst is more at lower VHSV and decreases as the VHSV increases, methane conversion is also expected to decrease as VHSV increases. If all the other parameters are fixed, a higher residence time leads to better conversion and the simple kinetic model developed in this study manages to highlight this important effect.

Conclusion

A 3D coupled numerical model for microwave assisted TCD of methane is developed. The temperature distribution identified hot spots in the upper and lower half of the catalyst. The concentration profiles for both CH_4 and H_2 predicted a linear change across the length of the reactor tube and correctly capture the catalyst deactivation over time as the reaction proceeds. The CH_4 conversion profiles at different temperatures and VHSV values show reasonable agreement with experimental data.

Acknowledgements

The authors would like to acknowledge the financial support by the UK Engineering and Physical Sciences Research Council (EPSRC) project grant: EP/K036548/2 and EP/M013162/1.

Appendix A. Supplementary data

Supplementary data related to this article can be found at http://dx.doi.org/10.1016/j.ijhydene.2016.09.126.

REFERENCES

[1] Panwar N, Kaushik S, Kothari S. Role of renewable energy sources in environmental protection: a review. Renew Sustain Energy Rev 2011;15(3):1513–24.
[2] Midilli A, Dincer I. Hydrogen as a renewable and sustainable solution in reducing global fossil fuel consumption. Int J Hydrogen Energy 2008;33(16):4209–22.
[3] Dufour J, Serrano D, Glvez J, Moreno J, Garca C. Life cycle assessment of processes for hydrogen production. Environmental feasibility and reduction of greenhouse gases emissions. Int J Hydrogen Energy 2009;34(3):1370–6.
[4] Muradov N. How to produce hydrogen from fossil fuels without CO2 emission. Int J Hydrogen Energy 1993;18(3):211–5.
[5] Muradov N. CO2-free production of hydrogen by catalytic pyrolysis of hydrocarbon fuel. Energy Fuels 1998;12(1):41–8.
[6] Ashok J, Kumar S, Venugopal A, Kumari V, Tripathi S, Subrahmanyam M. COx free hydrogen by methane decomposition over activated carbons. Catal Commun 2008;9(1):164–9.
[7] Serrano D, Botas J, Fierro J, Guil-Lpez R, Pizarro P, Gmez G. Hydrogen production by methane decomposition: origin of the catalytic activity of carbon materials. Fuel 2010;89(6):1241–8.
[8] Zhang J, Jin L, Liu S, Xun Y, Hu H. Mesoporous carbon prepared from direct coal liquefaction residue for methane decomposition. Carbon 2012;50(3):952–9.
[9] Moliner R, Suelves I, Lzaro M, Moreno O. Thermocatalytic decomposition of methane over activated carbons: influence of textural properties and surface chemistry. Int J Hydrogen Energy 2005;30(3):293–300.
[10] Kim M, Lee E, Jun J, Kong S, Han G, Lee B, et al. Hydrogen production by catalytic decomposition of methane over activated carbons: kinetic study. Int J Hydrogen Energy 2004;29(2):187–93.
[11] Krzyzynski S, Kozlowski M. Activated carbons as catalysts for hydrogen production via methane decomposition. Int J Hydrogen Energy 2008;33(21):6172–7.
[12] Muradov N. Catalysis of methane decomposition over elemental carbon. Catal Commun 2001;2(3–4):89–94.
[13] Bai Z, Chen H, Li B, Li W. Catalytic decomposition of methane over activated carbon. J Anal Appl Pyrolysis 2005;73(2):335–41.
[14] Shen Y, Lua A. A trimodal porous carbon as an effective catalyst for hydrogen production by methane decomposition. J Colloid Interface Sci 2016;462:48–55.
[15] Appleton T, Colder R, Kingman S, Lowndes I, Read A. Microwave technology for energy-efficient processing of waste. Appl Energy 2005;81(1):85–113.
[16] Fidalgo B, Domnguez A, Pis J, Menndez J. Microwave-assisted dry reforming of methane. Int J Hydrogen Energy 2008;33(16):4337–44.
[17] Mushtaq F, Mat R, Ani F. A review on microwave assisted pyrolysis of coal and biomass for fuel production. Renew Sustain Energy Rev 2014;39:555–74.
[18] Durka T, Stefanidis G, Van Gerven T, Stankiewicz A. Microwave-activated methanol steam reforming for hydrogen production. Int J Hydrogen Energy 2011;36(20):12843–52.
[19] Perry W, Datye A, Prinja A, Brown L, Katz J. Microwave heating of endothermic catalytic reactions: reforming of methanol. AIChE J 2002;48(4):820–31.
[20] Cooney DO, Xi Z. Production of hydrogen from methane and methane/steam in a microwave irradiated char-loaded reactor. Fuel Sci Technol Int 1996;14(8):1111–41.
[21] Dominguez A, Fidalgo B, Fernndez Y, Pis J, Menndez J. Microwave-assisted catalytic decomposition of methane over activated carbon for CO2-free hydrogen production. Int J Hydrogen Energy 2007;32(18):4792–9.
[22] Robinson J, Dodds C, Stavrinides A, Kingman S, Katrib J, Wu Z, et al. Microwave pyrolysis of biomass: control of process parameters for high pyrolysis oil yields and enhanced oil quality. Energy Fuels 2015;29(3):1701–9.
[23] Chen W-H, Cheng T-C, Hung C-I, Lin B-J. Chemical reactions and kinetics of a low-temperature water gas shift reaction heated by microwaves. Int J Hydrogen Energy 2012;37(1):276–89.
[24] Deng W, Su Y, Liu S, Shen H. Microwave-assisted methane decomposition over pyrolysis residue of sewage sludge for hydrogen production. Int J Hydrogen Energy 2014;39(17):9169–79.
[25] Mathe NR, Scriba MR, Coville NJ. Methanol oxidation reaction activity of microwave-irradiated and heat-treated Pt/Co and Pt/Ni nano-electrocatalysts. Int J Hydrogen Energy 2014;39(33):18871–81.
[26] Horikoshi S, Kamata M, Sumi T, Serpone N. Selective heating of Pd/AC catalyst in heterogeneous systems for the microwave-assisted continuous hydrogen evolution from organic hydrides: temperature distribution in the fixed-bed reactor. Int J Hydrogen Energy 2016;41(28):12029–37.
[27] Li H, Li X, Liu L, Li K, Wang X, Li H. Experimental study of microwave-assisted pyrolysis of rice straw for hydrogen production. Int J Hydrogen Energy 2016;41(4):2263–7.
[28] Matei-Rutkovska F, Postole G, Rotaru C, Florea M, Prvulescu V, Gelin P. Synthesis of ceria nanopowders by microwave-assisted hydrothermal method for dry reforming of methane. Int J Hydrogen Energy 2016;41(4):2512–25.
[29] Chen W-H, Liou H-J, Hung C-I. A numerical approach of interaction of methane thermocatalytic decomposition and microwave irradiation. Int J Hydrogen Energy 2013;38(30):13260–71.
[30] Fidalgo B, Menndez J. Study of energy consumption in a laboratory pilot plant for the microwave-assisted CO 2 reforming of CH 4. Fuel Process Technol 2012;95:55–61.
[31] Methane MSDS Sheet. Praxair, Inc.; 2016 [Online; accessed 29- 544 January-2016].
[32] Wang L, Wang RZ, Lu ZS, Chen CJ, Wang K, Wu J. The performance of two adsorption ice making test units using activated carbon and a carbon composite as adsorbents. Carbon 2006;44:26712680.
[33] CPL. Filtracarb FY5 12 x 30 US Datasheet [Online; Accessed 29 January 2016]. 2016.
[34] Martinez I. Thermo-optical properties [Online; Accessed 29 January 2016]. 2016.
[35] COMSOL. COMSOL 5.0 RF module library manual. 2015.
[36] Atwater JE, Wheeler Jr RR. Complex permittivities and dielectric relaxation of granular activated carbons at microwave frequencies between 0.2 and 26 GHz. Carbon 2003;41:18011807.
[37] Atwater JE, Wheeler Jr RR. Microwave permittivity and dielectric relaxation of a high surface area activated carbon. Appl Phys A Mater Sci Process 2004;79:125–9.
[38] Dawson EA, Parkes GMB, Barnes PA, Bond G, Mao R. The regeneration of microwave-induced plasma in granular active carbons under fluidised bed conditions. Carbon 2008;46:220–8.
[39] Jia B, Wang L. Preparation of microwave absorbing Ni-based activated carbon by electroless plating with Pd-free activation. Bioresources 2010;5:2248–57.
[40] Chandrasekaran R, Soneda Y, Yamashita J, Kodama M, Hatori H. Preparation and electrochemical performance of activated carbon thin films with polyethylene oxide-salt addition for electrochemical capacitor applications. J Solid State Electrochem 2008;12:13491355.
[41] Abbas H, Daud W. Deactivation of palm shell-based activated carbon catalyst used for hydrogen production by thermocatalytic decomposition of methane. Int J Hydrogen Energy 2009;34(15):6231–41.

Please cite this article in press as: Gadkari S, et al., Numerical analysis of microwave assisted thermocatalytic decomposition of methane, International Journal of Hydrogen Energy (2016), http://dx.doi.org/10.1016/j.ijhydene.2016.09.126